Experimental Parasitology 127 (2011) 249–259

Contents lists available at ScienceDirect

Experimental Parasitology

journal homepage: www.elsevier.com/locate/yexpr

Trypanosoma cruzi: Multiple actin isovariants are observed along different developmental stages

Ana María Cevallos [a,*], Yayoi X. Segura-Kato [a], Horacio Merchant-Larios [b], Rebeca Manning-Cela [d], Luis Alberto Hernández-Osorio [d,e], Claudia Márquez-Dueñas [d], Javier R. Ambrosio [c], Olivia Reynoso-Ducoing [c], Roberto Hernández [a]

[a] Departamento de Biología Molecular y Biotecnología, Universidad Nacional Autónoma de México, Apartado Postal 70-228, México, DF, Mexico
[b] Departamento de Biología Celular y Fisiología del Instituto de Investigaciones Biomédicas, Universidad Nacional Autónoma de México, Apartado Postal 70-228, México, DF, Mexico
[c] Departamento de Microbiología y Parasitología de la Facultad de Medicina, Universidad Nacional Autónoma de México, Apartado Postal 4510, México, DF, Mexico
[d] Departamento de Biomedicina Molecular, Centro de Investigación y de Estudios Avanzados del IPN, Apartado Postal 14–740, 07000 México, DF, Mexico
[e] Facultad de Medicina y Cirugía, Universidad Autónoma Benito Juárez de Oaxaca, Oaxaca, Mexico

ARTICLE INFO

Article history:
Received 15 February 2010
Received in revised form 12 July 2010
Accepted 3 August 2010
Available online 9 August 2010

Keywords:
Trypomastigote
Epimastigote
Amastigote
Kinetoplastid
Trypanosomatid
Actin isoforms
Actin-like protein
Actin-related protein

ABSTRACT

The expression and biological role of actin during the *Trypanosoma cruzi* life cycle remains largely unknown. Polyclonal antibodies against a recombinant *T. cruzi* actin protein were used to confirm its expression in epimastigotes, trypomastigotes, and amastigotes. Although the overall levels of expression were similar, clear differences in the subcellular distribution of actin among the developmental stages were identified. The existence of five actin variants in each developmental stage with distinct patterns of expression were uncovered by immunoblotting of protein extracts separated 2D-SDS gels. The isoelectric points of the actin variants in epimastigotes ranged from 4.45 to 4.9, whereas they ranged from 4.9 to 5.24 in trypomastigotes and amastigotes. To determine if the actin variants found could represent previously unidentified actins, we performed a genomic survey of the *T. cruzi* GeneDB database and found 12 independent loci encoding for a diverse group of actins and actin-like proteins that are conserved among trypanosomatids.

1. Introduction

Trypanosoma cruzi, the causative agent of Chagas' disease, is a digenetic parasite that develops via a complex life cycle involving insect vectors and mammalian stages. This organism displays distinct morphological and functional life forms, and it alternates between replicative stages (epimastigotes in the vector midgut and amastigotes in vertebrate cells) and non-dividing but infective forms (metacyclic trypomastigotes in the hindgut and faeces of the vector, and bloodstream trypomastigotes in the mammalian host). To complete their life cycle, the parasites undergo profound morphological and physiological changes, which are triggered by modifications in the microenvironment that occur in the insect digestive tract and within the vertebrate host cells. The differences in cell shape reflect changes in the organisation of the cytoskeleton and ultrastructure of the parasite (Elias et al., 2007).

Microtubules and actin microfilaments are the two major components of the eukaryotic cell cytoskeleton. Actin is a highly conserved protein that plays an essential role in the structure and dynamics of most eukaryotic cells. Eukaryotic cells use over100 accessory proteins to maintain a pool of actin monomers, initiate polymerisation, restrict the length of actin filaments, regulate the assembly and turnover of actin filaments, and cross-link filaments into networks or bundles (Pollard and Cooper, 2009). In trypanosomatids, the cytoskeleton is atypical in that the major component is a subpellicular corset of microtubules (Kohl and Gull, 1998). The presence of actin has been demonstrated in all trypanosomatid species studied; however, it does not appear to polymerise into highly structured cytoskeletal microfilaments. Furthermore, trypanosomatid motility does not depend on actin and they do not exhibit the ruffles or pseudopodia seen in amoebae and metazoa or the myosin-based gliding motility of the Apicomplexa. Actomyosin may not even be necessary for cytokinesis in these organisms (Berriman et al., 2005). So far, the only demonstrated functional role of actin in these organisms is in endocytosis (Bogitsh et al., 1995; Garcia-Salcedo et al., 2004). Two genomic surveys have identified putative proteins capable of regulating the dynamics of the actin cytoskeleton in trypanosomatids (Berriman et al., 2005; De Melo et al., 2008). Although potential homologues

* Corresponding author. Fax: +52 5 5622 9212.
E-mail address: amcevallos@biomedicas.unam.mx (A.M. Cevallos).

0014-4894/$ - see front matter © 2010 Elsevier Inc. All rights reserved.
doi:10.1016/j.exppara.2010.08.003

of two myosin families and proteins involved in monomeric actin binding and actin filament nucleation were present, no homologues of proteins involved in the severing, bundling, and cross-linking of microfilaments were identified. Moreover, the dynactin complex was not found, suggesting a major loss in the ability for cross-talk between the actin and tubulin filament networks (Berriman et al., 2005). The presence of a multigenic family of actin-encoding genes was not addressed in either of these studies.

Our research group is interested in studying the function of actin in *T. cruzi* during its life cycle. As an initial approach, we used an *Acanthamoeba castellanii* actin gene as a probe to isolate and clone three copies of an actin gene; two copies were present on one allele and only one copy was present on the other allele (Cevallos et al., 2003). These three gene copies encode for identical proteins. In this study, we investigated the expression of actin in three developmental stages of the parasite with the aid of a polyclonal serum raised against a recombinant version of the *T. cruzi* actin protein. The presence of actin variants was demonstrated by immunoblotting of parasite extracts separated by 2D-SDS gels. An *in silico* search for putative actin variants identified a diverse family of actin and actin-like proteins in this parasite.

2. Materials and methods

2.1. Cells and parasites

NIH 3T3 fibroblasts were maintained in Dulbecco's minimal essential media (DMEM) supplemented with 10% foetal bovine serum (FBS), 1% glutamine, and 5 μg/ml of penicillin–streptomycin, at 37 °C in a humidified atmosphere containing 5% CO_2. Epimastigotes from the *T. cruzi* strain CL-Brener were grown at 28 °C in liver infusion tryptose medium (LIT) supplemented with 10% foetal calf serum and 0.1 mg/ml haemin (Camargo, 1964).

Fifty percent-confluent fibroblasts were infected with 2×10^6 CL-Brener mid-log-phase epimastigotes/ml resuspended in high-glucose DMEM (15 ml) supplemented with 2% foetal bovine sera (FBS) to get a parasite-host cell ratio of 10:1. The NIH 3T3 monolayers were washed every two days with high-glucose DMEM medium until non-adherent parasites were removed, and then fresh high-glucose DMEM plus 2% FBS was added. Trypomastigotes and cell-derived amastigotes were isolated from the supernatant of infected NIH 3T3 fibroblasts. The amastigotes were separated from trypomastigotes using the amastigote-specific antibody 2C2B6, which is specific for the Ssp-4 surface antigen of amastigotes (Andrews et al., 1987). It has been shown that these amastigote preparations do not contain more than 5% trypomastigotes and that the trypomastigote preparations do not have more than 5% amastigotes (Manning-Cela et al., 2001). For some experiments, NIH 3T3 fibroblasts were grown on coverslips, infected with trypomastigotes, and fixed at one week post-infection. Protein extracts from *Leishmania mexicana, Toxoplasma gondii,* and *Trichomonas vaginalis* were kindly donated by Dr. Rosalía Lira, Dr. Rafael Saavedra, and Dr. Imelda López-Villaseñor, respectively.

2.2. Expression and purification of a recombinant GST-actin fusion protein

The entire actin-coding region was subcloned from a previously isolated genomic clone containing two copies of the gene (Cevallos et al., 2003) (Genbank accession number AF494294). The open reading frame was amplified by PCR using the following primers: GTGGGATCCCCATGTCTGACGAAGAACAG and GTGGGATCCCTAAAA GCATTTGTTGTGC. The amplification product was then cloned in frame into the *Bam*HI site of the bacterial expression vector pGEX-3X (Promega, Madison, Wisconsin), sequenced, and then expressed it in *Escherichia coli* strain BL21 (DE3) as a GST-actin fusion protein.

A 1:50 bacterial dilution (from an overnight culture grown at 37 °C in Luria–Bertani media containing 100 μg/ml of ampicillin) was grown until the OD_{600} reached 0.5. The cultures were then induced for 3 h by the addition of isopropylthio-β-galactoside to a final concentration of 0.1 mM. The bacteria were pelleted at $4500 \times g$ at 4 °C for 20 min, resuspended in a lysozyme-containing buffer (100 μg/ml lysozyme in 20 mM Tris–HCl, pH 7.5, 1 mM ethylenediaminetetraacetic acid), and incubated for 30 min at room temperature (RT). Protease inhibitors (aprotinin and leupeptin, at a final concentration of 10 μg/ml each) and sodium N-lauroyl sarcosinate (final concentration of 1.5%) were added, and the suspension was incubated for 2 h at RT before completing the cell lysis by sonication. A soluble fraction was obtained by centrifugation at 12,000*g* for 10 min at 4 °C. Phosphate buffered saline, pH 7.2 (PBS, 10X) and Triton X-100 were added to the soluble fraction to a final concentration of 1X and 1%, respectively. The lysate was then loaded into a glutathione Sepharose 4B column, and the recombinant protein was eluted according to the manufacturer's instructions (Amersham Biosciences, London, UK). Since several contaminant proteins remained in the eluted fraction, a second purification was carried out. The proteins eluted from the column were separated by 10% sodium dodecyl sulphate–polyacrylamide gel electrophoresis (SDS–PAGE), stained with Coomassie blue, and the band corresponding to the recombinant fusion protein was cut from the gel and electroeluted. The electroeluted protein was dialysed overnight at 4 °C in 10 mM Tris–HCl, pH 8, 100 mM NaCl, and 10% glycerol. The protein was then concentrated by ultra filtration in Centricon 30 filter units (Millipore Corporation, Bedford, USA) and stored at −20 °C until use.

2.3. Production of rabbit anti-T. cruzi actin polyclonal antibodies

Purified recombinant actin (200 μg) in 1 ml of Freund's complete adjuvant was administered subcutaneously to a New Zealand White rabbit. Two booster doses (130 μg of protein in 1 ml of incomplete Freund's adjuvant per booster dose, subcutaneously) were administered at 4- or 5-week intervals. Pre-immune blood was collected from the marginal ear vein. Fifteen days after the last antigen boost, blood was obtained by terminal cardiac puncture. The blood was allowed to clot for 30 min and centrifuged at 5000*g* for 20 min, and the serum was then collected. Serum aliquots were kept at −70 °C until use. The immunisation protocol and housing conditions were approved by the local Bioethics Committee for Animal Research.

2.4. Separation of protein lysates from epimastigotes into soluble and insoluble fractions

Epimastigotes at the exponential phase of growth were harvested as previously described, washed, and then lysed in PBS containing 1% (v/v) Triton X-100 and protease inhibitors (aprotinin and leupeptin at a final concentration of 10 μg/ml each) for 15 min at 4 °C. The lysates were then centrifuged at 12,000*g* for 20 min at 4 °C, and the clear supernatants were collected as soluble fractions. The insoluble pellets were washed once with the above buffer and then centrifuged again at 12,000*g* for 20 min at 4 °C. The final pellets were resuspended in the same volume that was initially used to lyse the cells. Equal volumes of both the soluble and insoluble fractions were analysed for actin and tubulin by immunoblotting.

2.5. Sample solubilisation and protein concentration for 2-D gel electrophoresis

A protocol that has been successfully used to characterise the actin isoforms of *Taenia solium* cysticerci was modified as follows

(Ambrosio et al., 2003): parasites from the three developmental stages were washed twice with PBS and resuspended in a solubilisation solution (40 mM KCl, 1 mM $MgCl_2$, and 6.7 mM phosphate buffer, pH 7.4) containing a cocktail of protease inhibitors (Complete, Roche) at a concentration of 10^8 parasites/ml and then stored −70 °C until processing. The proteins were later precipitated in the presence of 10% trichloroacetic acid, and 20 mM 1,4-bis(sulfanyl)butane-2,3-diol (dithiothreitol) in cold acetone. The proteins were dissolved in 125 μl of rehydration solution (2% buffer for immobilized pH gradient gels 4–7, 7 M urea, 2 M thiourea, 4% 3-[(3-Cholamidopropyl)dimethylammonio] propanesulfonic acid, 60 mM dithiothreitol, and 0.002% bromophenol blue), and the protein concentration present in the samples was determined with the DC Protein Assay Kit II (Bio-Rad).

2.6. Isoelectric focusing

Sixty micrograms of protein were loaded onto 7-cm immobiline DryStrips, pH 4–7 (GE Healthcare) and incubated for 16 h at RT. Focusing was then performed using a Protean IEF cell unit (Bio-Rad) that was adjusted to 20 °C in several steps: (1) 250 V, 20 min, linear slope; (2) 4000 V, 120 min, linear slope; and (3) 4000 V, 10,000 V/hour, rapid slope.

2.7. 2-D electrophoresis

After isoelectrofocusing, the strips were incubated for 15 min at RT under continuous stirring in the presence of a sodium dodecyl sulphate (SDS) equilibration buffer (50 mM Tris-Base, pH 8.8, 6 M urea, 30% glycerol, 2% SDS, and 0.002% bromophenol blue) supplemented with 1% dithiothreitol. Later, the equilibrated strips were transferred to an SDS equilibration buffer supplemented with 2.5% iodoacetamide. The strips were recovered and melted with 0.5% agarose in preparative commercial precast minigels (NuPage 4–12% Bis-Tris Minigel, Invitrogen). Electrophoretic separations (2-D gels) were carried out according to the manufacturer's specifications using an XCell SureLock chamber for 40 min at 200 V at 4 °C in the presence of a commercial running buffer (NuPage MES SDS Running Buffer, Invitrogen) and a 0.25% NuPAGE antioxidant. Proteins were stained with Sypro Ruby (Molecular Probes).

2.8. Immunoblotting

Total parasite lysates were separated by 10% SDS–PAGE and transferred to a 0.5-μm nitrocellulose membrane according to standard protocols. Any unbound sites on the nitrocellulose membrane were blocked with PBS containing 5% normal goat sera (NGS) overnight at 4 °C with gentle shaking. The membrane was then incubated for 1 h at RT with shaking with a 1:8000 dilution of the anti-*T. cruzi* actin polyclonal serum (anti-Tc-actin serum) in 0.1% Tween-20 in PBS (PBS-T) with 2% NGS. At the end of the incubation period, the membrane was washed three times with PBS-T (30 min per wash) and then incubated for 1 h with horseradish peroxidase-labelled goat anti-rabbit IgG (ImmunoPure, Pierce) diluted in PBS-T with 2% NGS (1:50,000 v/v). The membrane was washed three times with PBS-T (3 min per wash), incubated in SuperSignal West Pico Chemiluminescent Substrate (Pierce), and then exposed to film and developed. To characterise the recombinant protein, antibodies against the C-terminal peptide of rabbit actin (C11 peptide, Ser-Gly-Pro-Ser-Ile-Val-His-Arg-Lys-Cys-Phe; Sigma–Aldrich, A2066) were used (1:100 dilution). In some studies, monoclonal antibodies against α-tubulin were used at a dilution of 1:30,000 (Amersham Life Science, N356).

For samples separated by 2D-electrophoresis, the proteins were transferred at 30 V for 1 h onto methanol-activated polyvinylidene difluoride Immobilon-P membranes (PVDF; Millipore) using a transfer buffer containing 0.25% NuPAGE antioxidant (Invitrogen). For the detection of actin, the membranes were incubated for 1 h at RT with the anti-Tc-actin serum that was previously diluted 1:6000 in 0.25% bovine serum albumin in PBS-T. The membranes were washed three times before adding the horseradish peroxidase-goat anti-rabbit IgG conjugate antibody (Zymed) diluted in 0.25% BSA in PBS-T (1:40,000 v/v). The membranes were incubated for 30 min and then washed for 24 h at RT with alternating changes of PBS-T and 0.1% Tween-20 in Tris-buffered saline. Finally, the enzymatic reaction was developed using the chemiluminescent substrate listed above.

A Chemi-doc XRS System (Bio-Rad) was used to acquire images of the immunoblot membranes. The acquired images were processed using the manufacturer's Quantity One 1-D Analysis Software, V. 4.6 (Bio-Rad) and PDQuest Advanced 2-D Analysis Software, V. 7.4 (Bio-Rad). Immunoblots were printed and scanned at a resolution of 2400 ppi. The images were processed in Adobe Photoshop CS for contrast before incorporation into the final figure.

2.9. Immunofluorescence microscopy

Parasites isolated at different developmental stages were washed two times for 5 min each with PBS, resuspended in 4% (w/v) paraformaldehyde in PBS, and allowed to adhere to the substrate during fixation for 30 min at RT. To analyse intracellular amastigotes, infected NIH 3T3 fibroblasts grown on coverslips were fixed with 4% paraformaldehyde (w/v) in PBS at 25 °C for 10 min and then washed as described above. Both types of fixed cells were permeabilised with 0.1% (v/v) Triton X-100 for 30 min and then blocked with 2% (w/v) bovine serum albumin in PBS for 2 h. The blocked cells were first incubated with primary antibodies (1:250 dilution) overnight at 4 °C and then labelled with goat anti-rabbit IgG Fluorescein-5-isothiocyanate (FITC)-tagged antibodies (1:200 dilution) for 30 min at RT in the dark. The preparations were mounted for fluorescence in Vectashield medium containing propidium iodide (Vector) to stain nucleic acids. The negative control samples were incubated with pre-immune rabbit serum instead of primary anti-serum. The samples were observed using a confocal microscope (LSM 5 Pascal, Zeiss) equipped with Argon-Krypton and Helium–Neon lasers and filters BP 450–490 and BP 546/12.

2.10. Sequence analysis and phylogenetic trees

The deduced aminoacid sequences of the actin and actin-like proteins of *T. cruzi* were aligned using the Clustal W2 algorithm at the European Bioinformatics Institute Web Site (Larkin et al., 2007). Validation of these sequences as belonging to the actin family of proteins was perfomed at the Conserved Domain Database at the The National Center for Biotechnology Information (Marchler-Bauer et al., 2009). Phylogenetic inference of aminoacid sequences set was performed under the optimal criterion of Maximum Parsimony and Neighbour Joining using PAUP* 4.0b10 (Swofford, 2002). For Maximum Parsimony trees, heuristic tree building algorithm with 100 search replicates was used to obtain the most parsimonious tree, random addition taxa sampling, tree-bisection-reconnection branch-swapping. Characters were treated as unordered, gaps as missing data. *Euglena gracilis* actin (accession No. AAC99646) was used as outgroup to root the tree.

3. Results

3.1. Anti-actin polyclonal antibodies recognise a ~44-kDa protein in T. cruzi epimastigotes

We cloned, expressed, and purified a *T. cruzi* recombinant actin as a 68-kDa GST-fusion protein in *E. coli* (Fig. 1A). Polyclonal

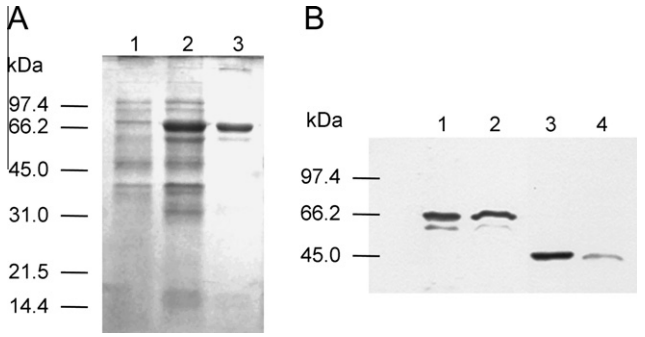

Fig. 1. Characterization of the recombinant *T. cruzi* actin. (A) Expression of *T. cruzi* actin in *E. coli*. The protein lysates were analysed by SDS–PAGE, and the gels were stained with Coomassie blue. Lane 1, uninduced cell lysates; lane 2, induced cell lysates; lane 3, eluate from glutathione Sepharose 4B column. (B) Immunoblots using commercial polyclonal antibodies against the C-terminal peptide of rabbit actin. Lane 1, induced *E. coli* protein lysate; lane 2, eluate from Sepharose B column; lane 3, NIH 3T3 fibroblasts lysate; lane 4, *T. cruzi* epimastigote cell lysate.

antibodies against a conserved C-terminal peptide of rabbit actin recognised the recombinant protein, as well as actin present in the protein lysates from mammalian cells and from *T. cruzi* epimastigotes (Fig. 1B), demonstrating that actin epitopes were present in the recombinant protein. However, the recognition of *T. cruzi* actin by the commercial antibody was poor; therefore, a polyclonal serum against the homologous *T. cruzi* actin protein was produced.

The purified GST-actin fusion protein was used for rabbit immunisation to obtain a polyclonal actin antibody. The anti-Tc-actin serum recognised a protein of approximately 44 kDa in epimastigote extracts (Fig. 2A). Commercial antibodies against the GST fragment of the protein did not recognise any *T. cruzi* protein by either immunoblot or immunofluorescence (data not shown). The antibody recognition of actin was not species-specific, as proteins of similar size were also detected in lysates from *L. mexicana* procyclics, *T. gondii* sporozoites, and *T. vaginalis* trophozoites (Fig. 2A). The sizes of the recognised proteins corresponded to the expected size of actin from each organism (Brugerolle et al., 1996; Dobrowolski et al., 1997; Sahasrabuddhe et al., 2004).

In some parasitic protozoa, such as *T. gondii* and *L. donovani,* the predominant form of actin is soluble (Dobrowolski et al., 1997; Sahasrabuddhe et al., 2004). In contrast, a previous study of actins in trypanosomatids suggested that in *Herpetomonas samuelpessoai* promastigotes and *T. cruzi* metacyclic trypomastigotes, actin is present in the insoluble fraction (Mortara, 1989). More recently, De Melo et al. (2008) detected actin only in the detergent-extracted soluble fraction, indicating that it was either in the monomeric form or in short filaments that had been dissociated from the microtubule cytoskeleton. To confirm these data, we performed fractionation studies using protein lysates of *T. cruzi* epimastigotes. Actin was readily detected in both the whole cell lysates and in the soluble fraction, but was present only in trace amounts in the insoluble fraction (Fig. 2B). As expected, the majority of α-tubulin was found in the insoluble fraction (Fig. 2B).

3.2. Actin is differentially expressed in three developmental stages of T. cruzi

Different life cycle forms of *T. cruzi* were subjected to immunoblot analysis using the anti-Tc-actin serum. These antibodies recognised the same 44-kDa band in trypomastigotes and amastigotes that was previously detected for epimastigotes, demonstrating the presence of actin in all developmental stages of the parasite (Fig. 2C).

The subcellular localization of actin in these developmental stages was investigated by indirect immunofluorescent antibody

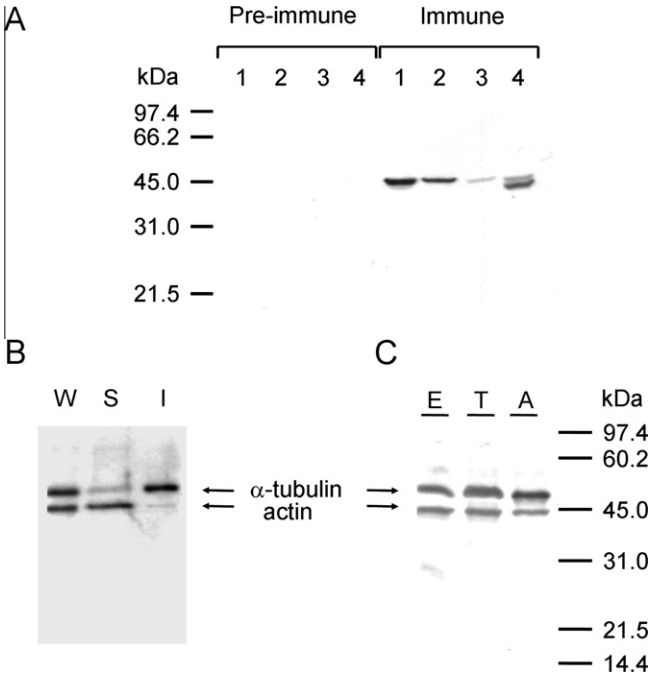

Fig. 2. Actin recognition by anti-*T. cruzi* actin antibodies. (A) Protein lysates (40 μg) from *T. cruzi* epimastigotes (1), *L. mexicana* procyclics (2), *T. gondii* sporozoites (3), and *T. vaginalis* tropohozoites (4) were probed with the anti-*T. cruzi* actin serum which recognised proteins with a size consistent with actin that were not recognised by the pre-immune serum. (B) Solubility of actin and tubulin of *T. cruzi* epimastigotes. Whole cell lysates (W) were fractionated into soluble (S) and insoluble (I) fractions and then probed by immunoblot using anti-Tc-actin serum and anti-α tubulin monoclonal antibodies. (C) Actin expression in three developmental stages of *T. cruzi*. Immunoblot of protein extracts from cells (5×10^6 parasites/lane; ~40 μg of protein) of different developmental stages with the anti-Tc-actin serum and with anti-α tubulin monoclonal antibodies (as loading control). E: epimastigotes, T: trypomastigotes and A: amastigotes.

staining of fixed cells. The pre-immune serum did not recognise *T. cruzi* epitopes in any of the developmental stages (Supplemental Fig. 1). We studied exponential and stationary phase epimastigotes because we had previously demonstrated that their actin mRNAs are stabilised during the stationary phase of growth (Cevallos et al., 2005). In both exponential and stationary phase epimastigotes, faint actin labelling was detected throughout the cell, consistent with the results of two previous studies that used heterologous antibodies (de Souza et al., 1983; Mortara, 1989). High levels of actin staining were also observed at the base of the flagellum near the presumed location of the flagellar pocket, and patches of staining were frequently seen along the flagellum (Fig. 3). These patches varied in number from cell to cell, but they were commonly present at the end of the flagellum, particularly in stationary phase epimastigotes. Magnification of the image showed that actin is concentrated at the edges of the flagellum, leaving a clearer zone inside (Fig. 3J–K).

In trypomastigotes, there appeared to be a low level of uniformly distributed actin labelling throughout the cell (Fig. 4 A and C). In cell-derived amastigotes obtained from the supernatant of infected cells, the actin localization was notably heterogeneous, with signals ranging from weak to intense and in some cases without apparent expression (Fig. 4 D and F). A detailed examination of actin distribution in the parasite demonstrated that actin tended to be present near the parasite edges, either diffusely (weakly or intensely) or as defined spots (1–3 per cell) (Fig. 4 G–J). The pattern of actin expression in intracellular amastigotes was more homogeneous when compared to cell-derived parasites (Fig. 5), but they still displayed the same pattern, with an apparent increase in actin

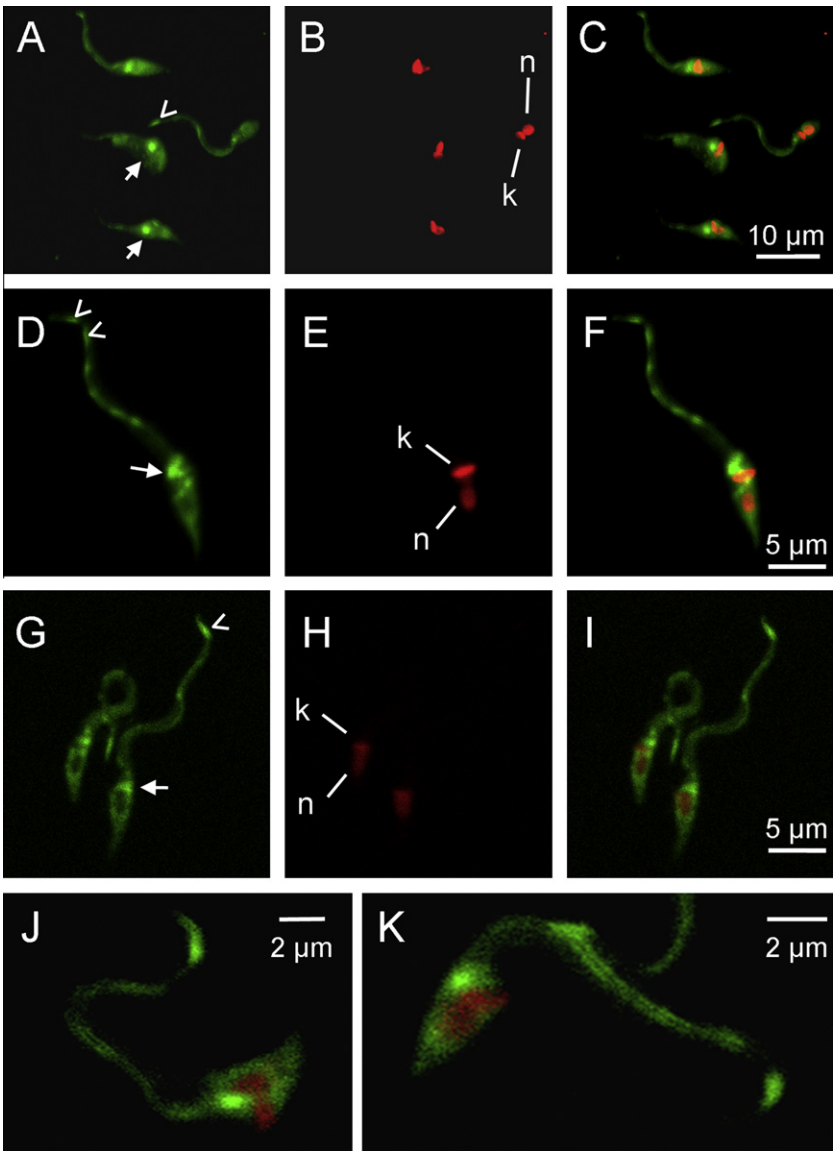

Fig. 3. Subcellular distribution of actin in epimastigotes. Confocal microscopy images of exponential phase (A–F) and stationary phase (G–K) epimastigotes. Figures (A), (D), and (G) correspond to actin expression detected with a FITC secondary antibody. The actin concentrations at the base of the flagellum are indicated by an arrow and actin patches are indicated by open arrowheads. Figures (B), (E), and (H) show the staining of nucleic acids with propidium iodide. The nucleus (n) and the kinetoplast (k) are marked. Figures (C), (F), and (I–K) show the merged images. In figures (J–K), enlarged figures are shown to demonstrate the pattern of actin distribution along the flagellum.

accumulation towards the parasite edges and the presence of defined spots (Fig. 5 M, O–S). Interestingly, some intermediate developmental stages could be observed, identified by their rounded cellular shape, the presence of a flagellum, and the relative position of the nucleus and kinetoplast (Hernandez-Osorio et al., 2010). In these parasites, actin expression was evident along the entire cell body and in the flagellum, where patches could also be observed (Fig. 5 J, L and N).Recognition of host actin by the anti-Tc-actin serum was consistently poor (Fig 5 A–C).

3.3. There are multiple T. cruzi actin isovariants with stage-specific patterns of expression

The presence of actin isoforms in each developmental stage was investigated by immunoblotting of solubilised protein extracts separated by 2D-gel electrophoresis. Two gels, run in parallel, were either stained with Sypro Ruby or transferred to PVDF membranes that were then used to detect the presence of actin isoforms (Fig. 6).

Analysis of the two-dimensional electrophoresis map of soluble proteins demonstrated the expression of several common proteins and the stage-specific expression of others, consistent with previously reported expression profiles (Paba et al., 2004). Interestingly, five actin signals from each stage were observed by immunoblot. Stage-specific signals with a narrow range of isoelectric points (pI) were observed in master images generated with PDQuest software using data derived from several processed membranes (Fig. 6). In epimastigotes, the pIs of the actin proteins ranged from 4.45 to 4.9, whereas in trypomastigotes and amastigotes, the pIs ranged from 4.9 to 5.24. There were also differences in the expression patterns; trypomastigotes expressed higher levels of the more basic proteins, whereas amastigotes expressed higher levels of the more acidic actin proteins (Fig. 6). Subtle differences may exist between the trypomastigote and amastigote actin proteins, since the calculated pIs were only identical for two of the five detected signals (T4 and A4 had a pI of 5.15; T5 and A5 had a pI of 5.24).

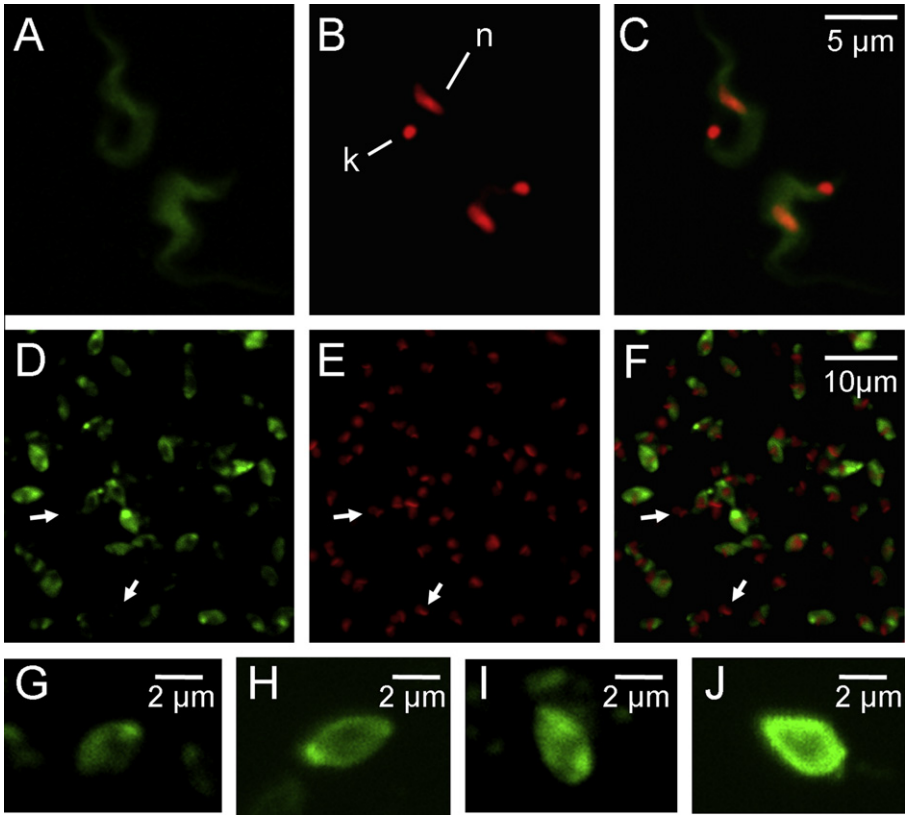

Fig. 4. Subcellular distribution of actin in trypomastigotes and amastigotes. Confocal microscopy images of trypomastigotes (A–C) and cell-derived amastigotes (D–J). Panels (A), (D), and (G–J) show actin expression detected with a FITC secondary antibody, demonstrating the diffuse distribution of actin in trypomastigotes (A) and the heterogeneous expression in amastigotes (D). Figures (B) and (E) show the staining of nucleic acids with propidium iodide. The nucleus (n) and kinetoplast (k) are marked. Figures (C) and (F) show the merged images. Arrows identify two parasites with no apparent actin expression. Amplification images demonstrating differences in actin distribution within individual amastigotes (G–J).

3.4. The T. cruzi genome encodes for numerous actin, actin-like and actin-related proteins

To determine whether the detected actin variants correspond to the expression of previously unidentified actin genes, a search of the *T. cruzi* genome project database was performed. Twelve loci annotated as actins, actin-like proteins, or actin-related proteins were identified (loci 1–12 in Table 1). This database includes the whole diploid genome of the hybrid *T. cruzi* strain CL-Brener. The majority of its loci are now identified as belonging to either the Esmeraldo or non-Esmeraldo haplotype (El-Sayed et al., 2005). The similarity of these new *T. cruzi* actins with the actin that we have previously reported (locus 1) ranges from 40–71%. The majority of these genes are present in *T. brucei* and *L. major*; however, we could not identify orthologues of two of the actin genes in either *T. brucei* or *L. major* (loci 2 and 3), or the orthologue of another actin gene in *T. brucei* (locus 4). As previously reported, genes for the actin nucleating proteins ARP-2 and ARP-3 are present (Ben Amar et al., 1988; De Melo et al., 2008). A member of the ARP-6 family is also present, and the *L. major* orthologue of this gene codes for a protein that is expressed in the nucleus of the parasite, as would be expected for a ARP-6 protein known to be involved in chromatin remodelling (Raza et al., 2007). All sequences were identified as actins with at least six algorithms (cd00012, smart00268, pfam00022, COG5277, PTZ00004, and PTZ00281). These analyses validate the annotation of all these genes as coding for members of the actin family of proteins.

A Clustal W alignment was performed to identify conserved motifs. The amino acid residues identified by the pfam00022 algorithm as putative ligand sites for ATP, profilin and gelsolin were not highly conserved in sequence but the majority of them were located in the same position (Supplemental Fig. 2). In general, there was little sequence conservation and changes were dispersed along the entire protein. In fact, only nine residues were identical in all the proteins studied, and only three of them are putative actin-ligand sites. However, many of the identified identical or conserved residues have been found to be important for actin function in other models (An and Mogami, 1996; Noguchi et al., 2010; Wertman et al., 1992). Interestingly, seven of the identical residues were glycines. It has been suggested that glycine residues provide flexibility to the actin molecule and that substitutions of critical glycine residues for other amino acids inhibit proper conformational changes and alter function (Noguchi et al., 2010). The Neighbour Joining tree obtained from these sequences and their orthologues in *T. brucei*, and *L. major* shows that each actin and actin-like protein is clustered irrespective of the species of protist, i.e., each protein is found in all these species (Fig. 7). However, when considering the different types of actin and actin-like proteins, they are not clustered together. Actins 2–4 are more similar to actin-like proteins than to actin 1. The same results are found when a Maximum Parsimony tree is generated (Supplemental Fig. 3). This tree shows that actins 2–4 are more closely related to actin-like proteins than to actin 1.

4. Discussion

In this study, we provide evidence from experimental and genomic *in silico* analysis for a diverse family of actins in *T. cruzi*. In addition, we demonstrate that the expression of actin variants changes during the development of this parasite. Previous

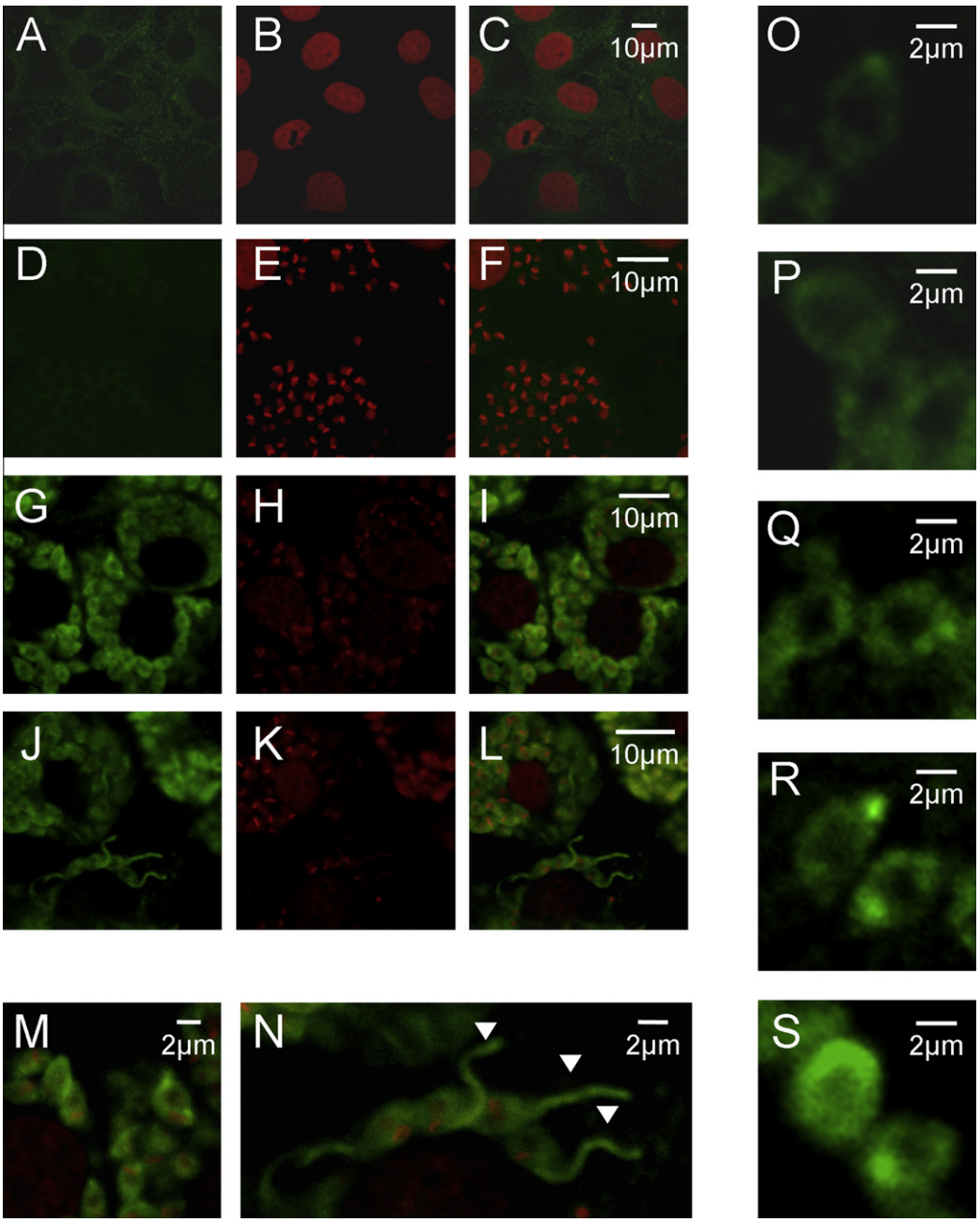

Fig. 5. Confocal microscopy of images from fibroblasts. Panels (A), (D), (G), (J) and (O–S) correspond to actin expression detected with a FITC secondary antibody; panels (B), (E), (H), and (K) correspond to the staining of nucleic acids with propidium iodide; and panels (C), (F), (I), and (L–N) correspond to merged images. Non-infected cells probed with our anti-Tc actin serum, demonstrating a weak recognition of mammalian actin (figures A–C). Infected cells probed with the pre-immune serum display a weak background (figures D–F). Infected cells probed with the anti-Tc actin serum; intense *T. cruzi* actin labelling is evident, with increased expression towards the parasite surface (figures G–N). An amplification of (I), in which the actin distribution in amastigotes can be appreciated in more detail (figure M). An amplification of the lower region of panel (L), where intermediate parasitic forms with an elongated flagellum are marked with arrowheads (figure M). Amplification images O–S demonstrate in more detail the differences in actin expression within intracellular amastigotes infecting other fibroblasts.

attempts to visualize microfilaments in trypanosomatids using phalloidin proved unsuccessful as their actins do not appear to bind it (Kapoor et al., 2008). The use of anti-sera raised against the actins of *T. brucei* and *L. donovani* has proved invaluable for the study of actin in these organisms (Garcia-Salcedo et al., 2004; Sahasrabuddhe et al., 2004). However, neither of these studies investigated the presence of actin variants. In *T. cruzi*, two previous studies using heterologous antibodies demonstrated the expression of actin in the epimastigote stage (de Souza et al., 1983; Mortara, 1989). In both reports, actin was found to be expressed throughout the cell body, but only one report clearly shows actin localization along the flagella (de Souza et al., 1983). In a recent study, immunofluorescence assays using a specific polyclonal antibody against a peptide from *T. cruzi* actin revealed punctate structures that were visible throughout the parasite body of epimastigotes, amastigotes, and trypomastigotes, with no observable differences among these parasite stages (De Melo et al., 2008). We have developed a polyclonal antibody against a recombinant actin from *T. cruzi* that recognises better the actins of protozoa than mammalian actins. Using this antibody, we demonstrated that overall actin expression is similar for all parasitic stages studied. However, we identified distinct differences in both its subcellular

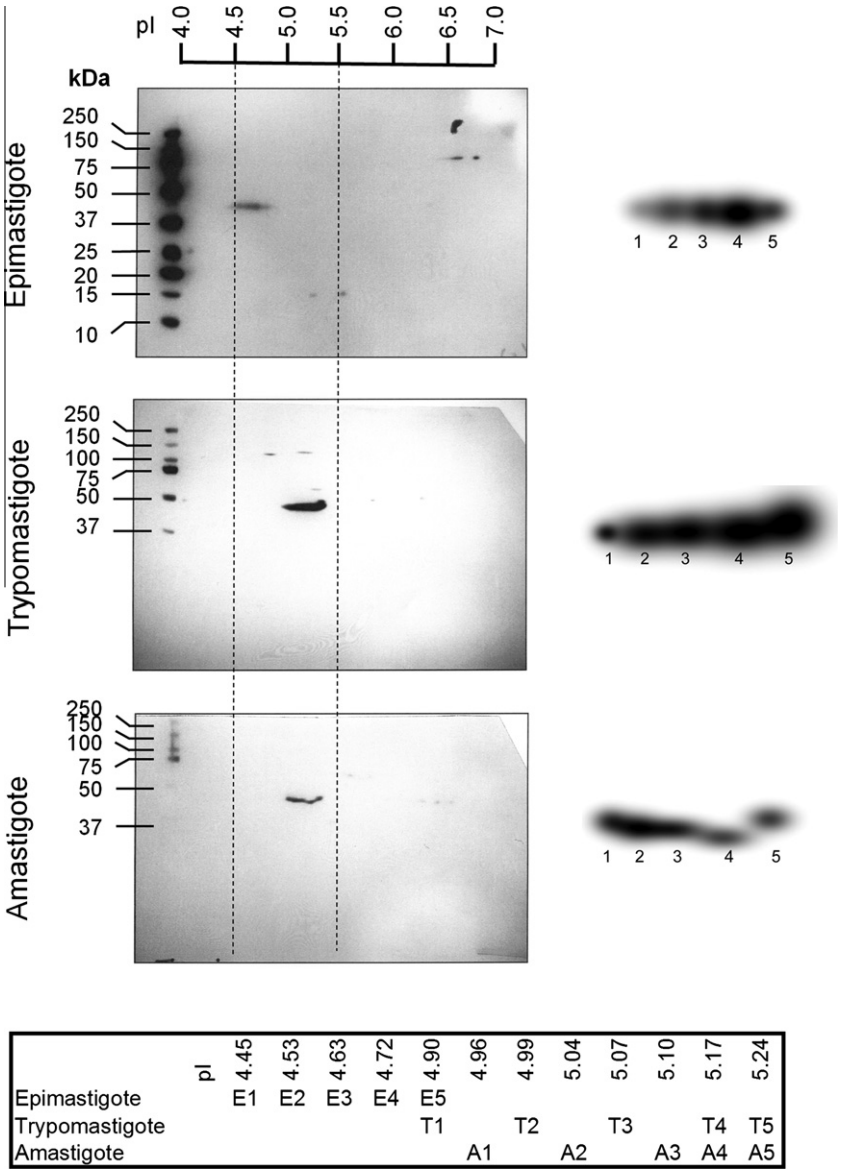

Fig. 6. Actin isoform expression in the three developmental stages. Protein extracts of solubilised proteins were separated by 2DE, transferred to PVDF membranes, and probed with the anti-Tc-actin serum. Precision Plus Protein Western standards (Bio-Rad) were used. The amplified insert shows the actin isoforms detected with anti-Tc-actin serum (images are not aligned according to their pIs). The interval delimited by the dotted-lines corresponds to the pI range where the actin spots were localized. The lower box depicts the estimated pI values determined for each actin spot and their distribution according with the developmental stages of the parasite.

distribution and in the type of actins expressed. The differences in the subcellular distribution of actin between our studies and those of de Melo et al. (2008) may be due to differences in the methodology employed, particularly in the development of the anti-actin sera. We employed a polyclonal antibody against the whole protein, while the previous study used an anti-serum raised against a small peptide corresponding to amino acids 50–63 of the actin protein previously reported by our group (Cevallos et al., 2003; De Melo et al., 2008). This peptide is situated in subdomain 2 of the protein (Sheterline et al., 1998), a region that is involved in potential actin-actin interactions, and therefore the reported anti-serum may not recognise epitopes that are unavailable in polymerised actin.

Actins are considered to be well conserved among eukaryotes. In virtually all eukaryotes, actins are encoded by a multigene family, with the only identified exception being yeast (Gallwitz and Seidel, 1980; Ng and Abelson, 1980). Differences between the amino acid sequences of actin variants in multicellular organisms are considered to be small, and the most dissimilar actins of plants and animals still share more than 85% sequence identity (Sheterline et al., 1998). However, the actins of protists have proved to be far less conserved, not only with respect to conventional actins of multicellular organisms, but also between actin variants in the same organism. For example, the percentage of identity between the diverse actin genes of *Paramecium tetraurelia* is as low as 28% (Sehring et al., 2007).

Differences in the subcellular distribution of actin variants or isoforms and the modulation of their expression during development have been well documented in plants and in animals (Khaitlina, 2001). In protists, examples of differences in the subcellular localization of actins due to the use of different actin variants have been reported. For example, *P. tetraurelia* expresses different sets of actins in specific cell compartments such as the cilia, cell cortex, and Golgi (Sehring et al., 2007). In *T. brucei*, an atypical actin (TryARP) that is only expressed in the flagellum has been characterised (Ersfeld and Gull, 2001); the orthologue of this actin in *T. cruzi* is encoded by locus 7 (Table 1). Changes in the pattern of actin expression during development have also been reported. In

Table 1
Actin and actin-like proteins of *T. cruzi*.

Locus	*T. cruzi* locus tag	Annotation	Protein ID	Identity (I) Similarity (+)	*T. brucei* Orthologue (protein ID)	*L. major* Orthologue (protein ID)	MW[a]	pI[a]	# aa	Haplotype	Chr[b]
1[c]	Tc00.1047053510571.30	Actin, putative	AAP97326	I = 100%	Tb9.211.0620	LmjF04.1230	42.0	5.5	376	non-E	8
	Tc00.1047053510571.39	Actin, putative	AAP97327	+ = 100%	(EAN76875)	(CAC22667)	42.0	5.5	376	non-E	
	Tc00.1047053510127.79	Actin, putative	AAP97329		Tb9.211.0630 (EAN76876)		42.0	5.5	376	Esmeraldo	
2	Tc00.1047053507969.50	Actin 2, putative	EAN87645	I = 51%	Not present	Not present	43.6	4.9	392	non-E	35
	Tc00.1047053507129.10	Actin 2, putative	EAN84193	+ = 71%			43.6	4.9	392	Esmeraldo	
3	Tc00.1047053510945.30	Actin, putative (actin 3)[d]	EAN86458	I = 39% + = 59%	Not present	Not present	42.8	5.3	390	E ≡ non-E	26
4	Tc00.1047053511463.4	actin, putative (actin 4)[d]	♦	I = 32%	Not present	LmjF35.0790				non-E	38
	Tc00.1047053503841.40	Actin, putative (actin 4)[d]	EAN85934	+ = 48%		(AAZ14306)	45.9	6.7	426	Esmeraldo	
5	Tc00.1047053506445.10	Actin-like protein 1, putative	♦	I = 30% + = 47%	Tb09.160.3960 (EAN76609)	LmjF15.1330 (CAJ03361)				non-E	7
	Tc00.1047053508277.330	Actin-like protein 1, putative	EAN98440				46.7	6.0	422	Esmeraldo	
6	Tc00.1047053508257.50	Actin-like protein 2, putative	EAN97086	I = 22% + = 42%	Tb927.4.980 (AAX80912)	LmjF34.3760 (CAJ08098)	41.1	5.4	372	non-E	34
	Tc00.1047053506405.30	Actin-like protein 2, putative	EAN90886				41.1	5.4	372	Esmeraldo	
7[e]	Tc00.1047053511857.50	Actin-like protein 3, putative	EAN87907	I = 33% + = 52%	Tb11.02.1380 (EAN79355)	LmjF13.0950 (CAJ02872)	47.5	5.5	428	non-E	14
	Tc00.1047053506733.50	Actin-like protein 3, putative	EAN92324				47.6	5.5	428	Esmeraldo	
8	Tc00.1047053509747.70	Actin-like protein 4, putative	EAN90479	I = 34% + = 53%	Tb11.01.1870 (EAN79963)	LmjF36.3310 (CAJ09294)	42.1	5.6	381	non-E	16
	Tc00.1047053510719.110	Actin-like protein 4, putative	EAN97339				42.2	5.7	381	Esmeraldo	
9	Tc00.1047053508153.600	Actin-like protein 5, putative	EAO00237	I = 26% + = 41%	Tb927.3.3020 (AAX79472)	LmjF29.2740 (AAZ09731)	35.3	6.0	327	Non-E	36
	Tc00.1047053506695.10	Actin-like protein 5, putative	EAN84931				35.3	6.0	327	Esmeraldo	
10	Tc00.1047053508899.110	Actin-related protein 2, putative	EAN93797	I = 36% + = 57%	Tb927.10.15800 (EAN78938)	LmjF19.1200 (CAJ07211)	45.2	6.2	403	non-E	40
	Tc00.1047053511361.40	Actin-related protein 2, putative	EAN87119				45.1	6.3	403	Esmeraldo	
11	Tc00.1047053503913.20	Actin-related protein 3, putative	EAN83141	I = 34% + = 53%	Tb09.160.3850 (EAN76600)	LmjF15.1360 (CAJ03366)	47.5	5.5	416	non-E	7
	Tc00.1047053508277.260	Actin-related protein 3, putative	EAN98434				47.5	5.5	416	Esmeraldo	
12[f]	Tc00.1047053510121.30	Member of ARP6 family	EAN94613	I = 22%	Tb10.70.5830	LmjF21.0230	54.9	6.9	500	non-E	5
	Tc00.1047053508951.29	Member of ARP6 family	EAN87149	+ = 40%	(EAN77627)	(CAJ03824)	54.8	7.2	500	Esmeraldo	

[a] MW and pI are theoretical; values were derived from the *T. cruzi* deduced amino acid sequence of the annotated genes.
[b] Chr = chromosome number.
[c] This actin locus contains two copies of the gene on one allele and one copy on the second allele (Cevallos et al., 2003).
[d] These actins were annotated in the genome only as actins. In this paper we labelled as actin 3 and actin 4.
[e] The *T. brucei* orthologue also known as TryARP has been characterised as a flagellar actin-related protein (Ersfeld and Gull, 2001).
[f] It has been shown that the *Leishmania* protein is expressed in the nucleolus as it would be expected for a member of the ARP6 family of proteins (Raza et al., 2007).
♦ The sequences corresponding to these genes are incomplete.

Plasmodium falciparum, an actin variant (pf-actin II) is only expressed in the sexual stages of the parasite (Wesseling et al., 1989). Actin isoforms that differ due to post-translational modifications have also been described. For example, in *Dictyostelium discoideum*, the pattern of actin isoform expression varies during development, with high levels of the phosporylated variant in spores (Kishi et al., 1998).

The occurence of a diverse family of actin and actin-like proteins in *T. cruzi* was unexpected. The Maximum Parsimony tree suggests that most of these proteins were present in the ancestral lineages of *Leishmania* and *Trypanosoma,* before the diversification of both genera. Actin 2 and 3 appeared only in *T. cruzi* whereas actin 4 was probably present in the three lineages (and their ancestors) and was secondary lost in *T. brucei*.

With the exception of actins at loci 2 and 3, all of the theoretical actin pIs (including the actin used to produce the anti-serum) are more basic than the experimentally determined pIs of the actin spots found in this study. This lack of correlation is not unexpected as differences of up to one pI unit may occur when comparing the theoretical and experimental pIs (Barrett et al., 2005). Based on their theoretical weight and pIs, the identified variants could be encoded at loci 1–3, 6, or 8. However, there is little sequence conservation between actin 1 used to produce the anti-Tc actin serum and these other actin and actin-like proteins. A certain degree of cross-reactivity may occur with actin 2 that has a 51% identity to actin 1 (Table 1). The 2D gel approach is particularly powerful for identification of protein isoforms that result from charged post-translational modifications, such as phosphorylation and sulfation (which add charge), or acetylation (which neutralize charge), among others (Friedman et al., 2009). These types of modifications cannot be inferred from the genome sequence data, are frequently reversible and their expression depend on the internal and external conditions of the cell. Among the known modifications of actin that may explain the changes in pI found in our study are acetylations and phosphorylations. The N-terminus of actins is generally processed by the removal of one or two amino acids followed by the irreversible addition of an acetyl group to the α-amino group of an acidic residue (Sheterline et al., 1998). The ε-acetylation of internal lysines of actin has also been identified (Choudhary et al., 2009; Kim et al., 2006). Actin phosphorylations of serines,

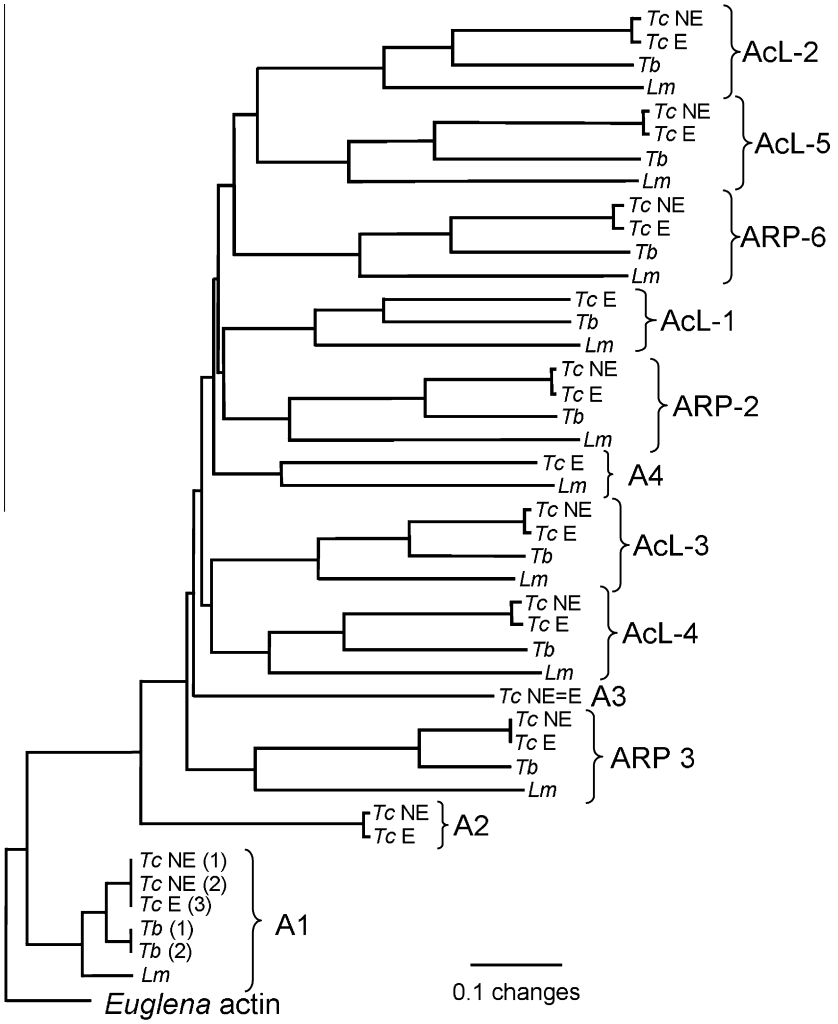

Fig. 7. Neighbour joining tree of trypanosomatid actins, actin-related and actin-like proteins. *E. gracilis* actin was used as outgroup to root the tree. Abbreviations: A = actin; AcL = actin-like protein; ARP = actin-related protein; Tc = *T. cruzi*; NE = non-Esmeraldo haplotype; E = Esmeraldo haplotype; Tb = *T. brucei*; and Lm = *L. major*. A1 has more than one copy in *T. cruzi* and *T. brucei* the corresponding copy number is in brackets.

threonines or tyrosines have been well documented (Gu et al., 2003; Kishi et al., 1998; Shirai et al., 2006). Other post-translational modifications found in actins include methylation, oxidation, S-nitrosylation, carbonylation and glutathionylation (Banan et al., 2000; Lu et al., 2009; Milzani et al., 1997; Nyman et al., 2002; Pizarro and Ogut, 2009). All these modifications are thought to play a role in the regulation of actin dynamics. It is likely that the changes of isoelectric point pattern among the parasite developmental stages identified in this study are related to the cumulative effect of multiple post-translational modifications in the net charge of actin. These findings suggest that actin has different physiological roles throughout the life cycle of *T. cruzi*.

In conclusion, in this study we have provided experimental and *in silico* evidence for the presence of actin isovariants in *T. cruzi*. We observed clear differences in the pattern of expression of actins recognised by our antibody in each parasite stage. It remains to be determined whether the differences in the variant types expressed in each stage are due to the cross-reactivity of our serum with other actins of similar size and pI, or whether these differences are due to post-translational modifications known to affect actin. The presence of different actin variants may provide trypanosome cells with a molecular system to regulate potential different functions of actin in the absence of a complex repertoire of actin-binding proteins. Further studies are required to address the nature and function of these variants.

Acknowledgments

We are very grateful to Dr. Gerardo Perez Ponce de León for his valuable help in the analysis of the phylogenetic trees. We thank René Escalona Mujica and Juliana Herrera for general technical assistance. This work was supported by grants IN213906 and IX222504, from DGAPA (PAPIIT) Universidad Nacional Autónoma de México and grant 79815 from CONACYT awarded to A.M. Cevallos; grant IN216107 from DGAPA (PAPIIT) Universidad Nacional Autónoma de México awarded to J. Ambrosio and CONACYT grants 42862 and 60152 awarded to R.G. Manning-Cela.

Appendix A. Supplementary data

Supplementary data associated with this article can be found, in the online version, at doi:10.1016/j.exppara.2010.08.003.

References

Ambrosio, J.R., Reynoso-Ducoing, O., Hernandez-Sanchez, H., Correa-Pina, D., Gonzalez-Malerva, L., Cruz-Rivera, M., Flisser, A., 2003. Actin expression in *Taenia solium* cysticerci (cestoda): tisular distribution and detection of isoforms. Cell Biology International 27, 727–733.

An, H.S., Mogami, K., 1996. Isolation of 88F actin mutants of *Drosophila melanogaster* and possible alterations in the mutant actin structures. Journal of Molecular Biology 260, 492–505.

Andrews, N.W., Hong, K.S., Robbins, E.S., Nussenzweig, V., 1987. Stage-specific surface antigens expressed during the morphogenesis of vertebrate forms of *Trypanosoma cruzi*. Experimental Parasitology 64, 474–484.

Banan, A., Zhang, Y., Losurdo, J., Keshavarzian, A., 2000. Carbonylation and disassembly of the F-actin cytoskeleton in oxidant induced barrier dysfunction and its prevention by epidermal growth factor and transforming growth factor alpha in a human colonic cell line. Gut 46, 830–837.

Barrett, J., Brophy, P.M., Hamilton, J.V., 2005. Analysing proteomic data. International Journal for Parasitology 35, 543–553.

Ben Amar, M.F., Pays, A., Tebabi, P., Dero, B., Seebeck, T., Steinert, M., Pays, E., 1988. Structure and transcription of the actin gene of *Trypanosoma brucei*. Molecular and Cellular Biology 8, 2166–2176.

Berriman, M., Ghedin, E., Hertz-Fowler, C., Blandin, G., Renauld, H., Bartholomeu, D.C., Lennard, N.J., Caler, E., Hamlin, N.E., Haas, B., Bohme, U., Hannick, L., Aslett, M.A., Shallom, J., Marcello, L., Hou, L., Wickstead, B., Alsmark, U.C., Arrowsmith, C., Atkin, R.J., Barron, A.J., Bringaud, F., Brooks, K., Carrington, M., Cherevach, I., Chillingworth, T.J., Churcher, C., Clark, L.N., Corton, C.H., Cronin, A., Davies, R.M., Doggett, J., Djikeng, A., Feldblyum, T., Field, M.C., Fraser, A., Goodhead, I., Hance, Z., Harper, D., Harris, B.R., Hauser, H., Hostetler, J., Ivens, A., Jagels, K., Johnson, D., Johnson, J., Jones, K., Kerhornou, A.X., Koo, H., Larke, N., Landfear, S., Larkin, C., Leech, V., Line, A., Lord, A., Macleod, A., Mooney, P.J., Moule, S., Martin, D.M., Morgan, G.W., Mungall, K., Norbertczak, H., Ormond, D., Pai, G., Peacock, C.S., Peterson, J., Quail, M.A., Rabbinowitsch, E., Rajandream, M.A., Reitter, C., Salzberg, S.L., Sanders, M., Schobel, S., Sharp, S., Simmonds, M., Simpson, A.J., Tallon, L., Turner, C.M., Tait, A., Tivey, A.R., Van Aken, S., Walker, D., Wanless, D., Wang, S., White, B., White, O., Whitehead, S., Woodward, J., Wortman, J., Adams, M.D., Embley, T.M., Gull, K., Ullu, E., Barry, J.D., Fairlamb, A.H., Opperdoes, F., Barrell, B.G., Donelson, J.E., Hall, N., Fraser, C.M., Melville, S.E., El-Sayed, N.M., 2005. The genome of the African trypanosome *Trypanosoma brucei*. Science 309, 416–422.

Bogitsh, B.J., Ribeiro-Rodrigues, R., Carter, C.E., 1995. In vitro effects of mannan and cytochalasin B on the uptake of horseradish peroxidase and [14C]sucrose by *Trypanosoma cruzi* epimastigotes. Journal of Parasitology 81, 144–148.

Brugerolle, G., Bricheux, G., Coffe, G., 1996. Actin cytoskeleton demonstration in *Trichomonas vaginalis* and in other trichomonads. Biology of the Cell 88, 29–36.

Camargo, E.P., 1964. Growth and differentiation in *Trypanosoma Cruzi*.I. Origin of metacyclic trypanosomes in liquid media. Revista do Instituto de Medicina Tropical de São Paulo 12, 93–100.

Cevallos, A.M., Lopez-Villasenor, I., Espinosa, N., Herrera, J., Hernandez, R., 2003. *Trypanosoma cruzi*: allelic comparisons of the actin genes and analysis of their transcripts. Experimental Parasitology 103, 27–34.

Cevallos, A.M., Perez-Escobar, M., Espinosa, N., Herrera, J., Lopez-Villasenor, I., Hernandez, R., 2005. The stabilization of housekeeping transcripts in *Trypanosoma cruzi* epimastigotes evidences a global regulation of RNA decay during stationary phase. FEMS Microbiology Letters 246, 259–264.

Choudhary, C., Kumar, C., Gnad, F., Nielsen, M.L., Rehman, M., Walther, T.C., Olsen, J.V., Mann, M., 2009. Lysine acetylation targets protein complexes and co-regulates major cellular functions. Science 325, 834–840.

De Melo, L.D., Sant'Anna, C., Reis, S.A., Lourenco, D., De Souza, W., Lopes, U.G., Cunha-e-Silva, N.L., 2008. Evolutionary conservation of actin-binding proteins in *Trypanosoma cruzi* and unusual subcellular localization of the actin homologue. Parasitology 135, 955–965.

de Souza, W., Meza, I., Martinez-Palomo, A., Sabanero, M., Souto-Padron, T., Meirelles, M.N., 1983. *Trypanosoma cruzi*: distribution of fluorescently labeled tubulin and actin in epimastigotes. Journal of Parasitology 69, 138–142.

Dobrowolski, J.M., Niesman, I.R., Sibley, L.D., 1997. Actin in the parasite *Toxoplasma gondii* is encoded by a single copy gene, ACT1 and exists primarily in a globular form. Cell Motility and the Cytoskeleton 37, 253–262.

El-Sayed, N.M., Myler, P.J., Bartholomeu, D.C., Nilsson, D., Aggarwal, G., Tran, A.N., Ghedin, E., Worthey, E.A., Delcher, A.L., Blandin, G., Westenberger, S.J., Caler, E., Cerqueira, G.C., Branche, C., Haas, B., Anupama, A., Arner, E., Aslund, L., Attipoe, P., Bontempi, E., Bringaud, F., Burton, P., Cadag, E., Campbell, D.A., Carrington, M., Crabtree, J., Darban, H., da Silveira, J.F., de Jong, P., Edwards, K., Englund, P.T., Fazelina, G., Feldblyum, T., Ferella, M., Frasch, A.C., Gull, K., Horn, D., Hou, L., Huang, Y., Kindlund, E., Klingbeil, M., Kluge, S., Koo, H., Lacerda, D., Levin, M.J., Lorenzi, H., Louie, T., Machado, C.R., McCulloch, R., McKenna, A., Mizuno, Y., Mottram, J.C., Nelson, S., Ochaya, S., Osoegawa, K., Pai, G., Parsons, M., Pentony, M., Pettersson, U., Pop, M., Ramirez, J.L., Rinta, J., Robertson, L., Salzberg, S.L., Sanchez, D.O., Seyler, A., Sharma, R., Shetty, J., Simpson, A.J., Sisk, E., Tammi, M.T., Tarleton, R., Teixeira, S., Van Aken, S., Vogt, C., Ward, P.N., Wickstead, B., Wortman, J., White, O., Fraser, C.M., Stuart, K.D., Andersson, B., 2005. The genome sequence of *Trypanosoma cruzi*, etiologic agent of Chagas disease. Science 309, 409–415.

Elias, M.C., da Cunha, J.P., de Faria, F.P., Mortara, R.A., Freymuller, E., Schenkman, S., 2007. Morphological events during the *Trypanosoma cruzi* cell cycle. Protist 158, 147–157.

Ersfeld, K., Gull, K., 2001. Targeting of cytoskeletal proteins to the flagellum of *Trypanosoma brucei*. Journal of Cell Science 114, 141–148.

Friedman, D.B., Hoving, S., Westermeier, R., 2009. Isoelectric focusing and two-dimensional gel electrophoresis. Methods in Enzymology 463, 515–540.

Gallwitz, D., Seidel, R., 1980. Molecular cloning of the actin gene from yeast *Saccharomyces cerevisiae*. Nucleic Acids Research 8, 1043–1059.

Garcia-Salcedo, J.A., Perez-Morga, D., Gijon, P., Dilbeck, V., Pays, E., Nolan, D.P., 2004. A differential role for actin during the life cycle of *Trypanosoma brucei*. The EMBO Journal 23, 780–789.

Gu, L., Zhang, H., Chen, Q., Chen, J., 2003. Calyculin A-induced actin phosphorylation and depolymerization in renal epithelial cells. Cell Motility and the Cytoskeleton 54, 286–295.

Hernandez-Osorio, L.A., Marquez-Duenas, C., Florencio-Martinez, L.E., Ballesteros-Rodea, G., Martinez-Calvillo, S., Manning-Cela, R.G., 2010. Improved method for in vitro secondary amastigogenesis of *Trypanosoma cruzi*: morphometrical and molecular analysis of intermediate developmental forms. Journal of Biomedicine and Biotechnology, 283842.

Kapoor, P., Sahasrabuddhe, A.A., Kumar, A., Mitra, K., Siddiqi, M.I., Gupta, C.M., 2008. An unconventional form of actin in protozoan hemoflagellate, Leishmania. Journal of Biological Chemistry 283, 22760–22773.

Khaitlina, S.Y., 2001. Functional specificity of actin isoforms. International Review of Cytology 202, 35–98.

Kim, S.C., Sprung, R., Chen, Y., Xu, Y., Ball, H., Pei, J., Cheng, T., Kho, Y., Xiao, H., Xiao, L., Grishin, N.V., White, M., Yang, X.J., Zhao, Y., 2006. Substrate and functional diversity of lysine acetylation revealed by a proteomics survey. Molecular Cell 23, 607–618.

Kishi, Y., Clements, C., Mahadeo, D.C., Cotter, D.A., Sameshima, M., 1998. High levels of actin tyrosine phosphorylation: correlation with the dormant state of Dictyostelium spores. Journal of Cell Science 111 (Pt 19), 2923–2932.

Kohl, L., Gull, K., 1998. Molecular architecture of the trypanosome cytoskeleton. Molecular and Biochemical Parasitology 93, 1–9.

Larkin, M.A., Blackshields, G., Brown, N.P., Chenna, R., McGettigan, P.A., McWilliam, H., Valentin, F., Wallace, I.M., Wilm, A., Lopez, R., Thompson, J.D., Gibson, T.J., Higgins, D.G., 2007. Clustal W and Clustal X version 2.0. Bioinformatics 23, 2947–2948.

Lu, J., Katano, T., Okuda-Ashitaka, E., Oishi, Y., Urade, Y., Ito, S., 2009. Involvement of S-nitrosylation of actin in inhibition of neurotransmitter release by nitric oxide. Molecular Pain 5, 58.

Manning-Cela, R., Cortes, A., Gonzalez-Rey, E., Van Voorhis, W.C., Swindle, J., Gonzalez, A., 2001. LYT1 protein is required for efficient in vitro infection by *Trypanosoma cruzi*. Infection and Immunity 69, 3916–3923.

Marchler-Bauer, A., Anderson, J.B., Chitsaz, F., Derbyshire, M.K., DeWeese-Scott, C., Fong, J.H., Geer, L.Y., Geer, R.C., Gonzales, N.R., Gwadz, M., He, S., Hurwitz, D.I., Jackson, J.D., Ke, Z., Lanczycki, C.J., Liebert, C.A., Liu, C., Lu, F., Lu, S., Marchler, G.H., Mullokandov, M., Song, J.S., Tasneem, A., Thanki, N., Yamashita, R.A., Zhang, D., Zhang, N., Bryant, S.H., 2009. CDD: specific functional annotation with the Conserved Domain Database. Nucleic Acids Research 37, D205–D210.

Milzani, A., DalleDonne, I., Colombo, R., 1997. Prolonged oxidative stress on actin. Archives of Biochemistry and Biophysics 339, 267–274.

Mortara, R.A., 1989. Studies on trypanosomatid actin. I. Immunochemical and biochemical identification. Journal of Protozoology 36, 8–13.

Ng, R., Abelson, J., 1980. Isolation and sequence of the gene for actin in *Saccharomyces cerevisiae*. Proceedings of the National Academy of Sciences of the United States of America 77, 3912–3916.

Noguchi, T.Q., Toya, R., Ueno, H., Tokuraku, K., Uyeda, T.Q., 2010. Screening of novel dominant negative mutant actins using glycine targeted scanning identifies G146V actin that cooperatively inhibits cofilin binding. Biochemical and Biophysical Research Communications 396, 1006–1011.

Nyman, T., Schuler, H., Korenbaum, E., Schutt, C.E., Karlsson, R., Lindberg, U., 2002. The role of MeH73 in actin polymerization and ATP hydrolysis. Journal of Molecular Biology 317, 577–589.

Paba, J., Santana, J.M., Teixeira, A.R., Fontes, W., Sousa, M.V., Ricart, C.A., 2004. Proteomic analysis of the human pathogen *Trypanosoma cruzi*. Proteomics 4, 1052–1059.

Pizarro, G.O., Ogut, O., 2009. Impact of actin glutathionylation on the actomyosin-S1 ATPase. Biochemistry 48, 7533–7538.

Pollard, T.D., Cooper, J.A., 2009. Actin, a central player in cell shape and movement. Science 326, 1208–1212.

Raza, S., Sahasrabuddhe, A.A., Gupta, C.M., 2007. Nuclear localization of an actin-related protein (ORF LmjF21.0230) in Leishmania+. Molecular and Biochemical Parasitology 153, 216–219.

Sahasrabuddhe, A.A., Bajpai, V.K., Gupta, C.M., 2004. A novel form of actin in Leishmania: molecular characterisation, subcellular localisation and association with subpellicular microtubules. Molecular and Biochemical Parasitology 134, 105–114.

Sehring, I.M., Reiner, C., Mansfeld, J., Plattner, H., Kissmehl, R., 2007. A broad spectrum of actin paralogs in *Paramecium tetraurelia* cells display differential localization and function. Journal of Cell Science 120, 177–190.

Sheterline, P., Clayton, J., Sparrow, J., 1998. Actin. Oxford University Press, Oxford.

Shirai, Y., Sasaki, N., Kishi, Y., Izumi, A., Itoh, K., Sameshima, M., Kobayashi, T., Murakami-Murofushi, K., 2006. Regulation of levels of actin threonine phosphorylation during life cycle of *Physarum polycephalum*. Cell Motility and the Cytoskeleton 63, 77–87.

Swofford, D.L., 2002. PAUP*. Phylogenetic analysis using parsimony (*and other methods), version 4.0b10. Sinauer Associates, Sunderland, MA.

Wertman, K.F., Drubin, D.G., Botstein, D., 1992. Systematic mutational analysis of the yeast ACT1 gene. Genetics 132, 337–350.

Wesseling, J.G., Snijders, P.J., van Someren, P., Jansen, J., Smits, M.A., Schoenmakers, J.G., 1989. Stage-specific expression and genomic organization of the actin genes of the malaria parasite *Plasmodium falciparum*. Molecular and Biochemical Parasitology 35, 167–176.